방사선방어학회지
제19권 제1호 1994

■ 論 文 ■

Monte Carlo Calculation of Thermal Neutron Flux Distribution for (n, γ) Reaction in Calandria

Soon-Young Kim, Jong-Kyung Kim, Kyo-Youn Kim*

Hanyang University
*Korea Atomic Energy Research Institute**

ABSTRACT

The MCNP 4.2 code was used to calculate the thermal neutron flux distributions for (n, γ)reaction in mainshell, annular plate, and subshell of the calandria of a CANDU 6 plant during operation. The thermal neutron flux distributions in calandria mainshell, annular plate, and subshell were in the range of $10^{11}\sim10^{13}$ neutrons/cm^2-sec which is somewhat higher than the previous estimates calculated by DOT 4.2 code. As an application to shielding analysis, photon dose rates outside the side and bottom shields were calculated. The resulting dose rates at the reactor accessible areas were below design target, 6 μSv/h. The methodology used in this study to evaluate the thermal neutron flux distribution for (n, γ)reaction can be applied to radiation shielding analysis of CANDU 6 type plants.

Key words: MCNP 4.2 code, thermal neutron flux distribution, (n, γ) reaction, calandria, photon dose rates

INTRODUCTION

Though the MCNP code[1] based on Monte Carlo method has been used very extensively and successfully over a decade in a wide variety of applications, radiation shielding calculation in CANDU reactors has not been carried out by using the code. Recently, the thermal neutron flux distributions for (n, γ)reaction[2] in mainshell, annular plate, and subshell of the calandria have been obtained by using the two-dimensional discrete ordinates transport code, DOT 4.2. Then the QAD-CG code has been used to calculate the photon dose rates at the accessible areas in CANDU 6 reactor. The DOT code uses space and angle discretization in two-dimensional geometry and group cross-section data. On the contrary, the MCNP code can simulate the three-dimensional reactor geometry

completely and use continuous cross-section data or discrete one. In addition, shielding calculation over entire reactor geometry can be done by using the code.

In this study, Monte Carlo calculations of thermal neutron flux distributions for (n, γ)reaction in calandria mainshell, annular plate, and subshell in a CANDU 6 reactor were carried out and the photon dose rates at the accessible areas such as main airlock area, new fuel loading area, and the stairway in the main lobby area are also calculated. The calculational model used in this work is based upon Point Lepreau power plant, a CANDU 6 reactor. The MCNP code version 4.2 was used.

Table 1. Fission neutron spectrum used in MCNP4.2 runs

Energy Range(eV)	Fraction of Neutrons per Fission
1.49E+7~1.22E+7	4.0489×10^{-4}
1.22E+7~1.11E+7	7.2582×10^{-4}
1.11E+7~6.07E+6	5.9696×10^{-2}
6.07E+6~3.68E+6	2.8362×10^{-1}
3.68E+6~2.23E+6	5.5141×10^{-1}
2.23E+6~1.35E+6	6.0629×10^{-1}
1.35E+6~8.21E+5	4.7288×10^{-1}
8.21E+5~4.98E+5	3.0088×10^{-1}
4.98E+5~3.02E+5	1.6975×10^{-1}
3.02E+5~1.83E+5	8.9190×10^{-2}
1.83E+5~6.74E+4	6.6967×10^{-1}
6.74E+4~4.09E+4	1.0663×10^{-2}
4.09E+4~2.48E+4	5.1082×10^{-2}
2.48E+4~1.50E+4	2.4337×10^{-3}
1.50E+4~0	

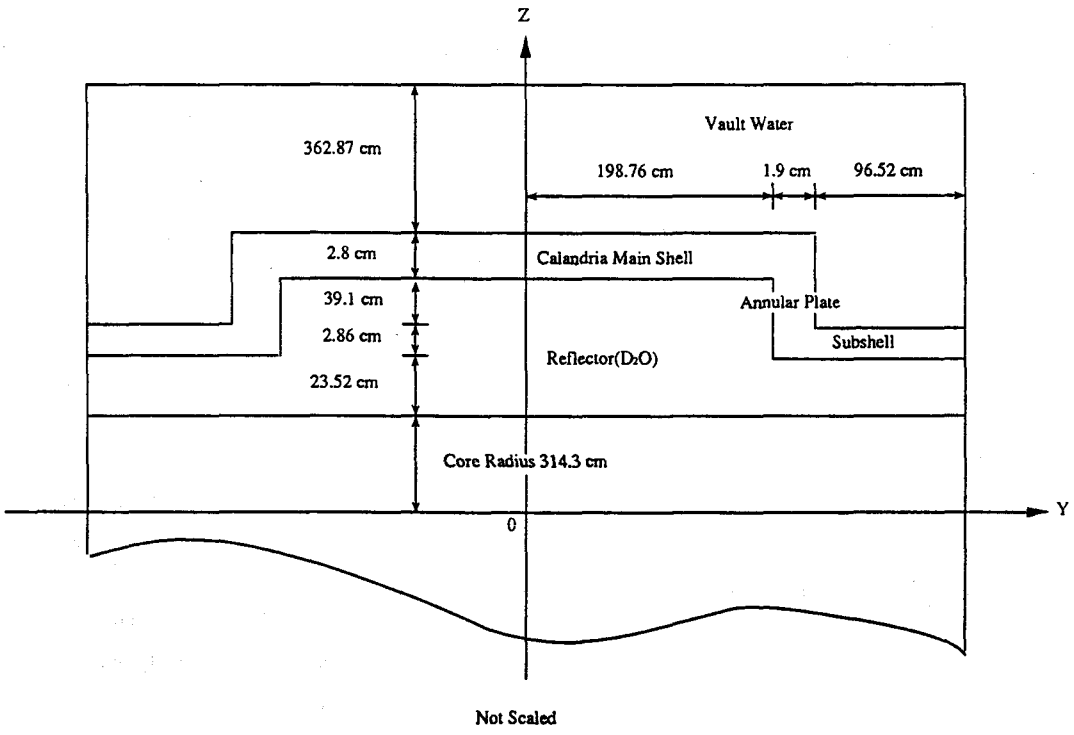

Figure 1. Cross-sectional view of calandria at X=0.

CALCULATION OF THERMAL NEUTRON FLUX DISTRIBUTIONS FOR (n, γ) REACTION IN CALANDRIA

The reactor core was divided into 15 cells to account the power output distributions in core. Time-average channel power distribution and time-average bundle power distributions[3] provided by the Point Lepreau power plant were used to determine the source sampling in each source cell for this calculation. The fission neutron spectrum from GAM II[4] was used for energy distribution of the source neutrons as shown in Table 1. Fission neutrons having energies below 0.015 MeV were ignored because of low yield.

The geometrical set up for the MCNP 4.2 calculation is shown in Figure 1 and the materials that constitute each region are given in Table 2. The subshell and the annular plate were divided into 8 regions horizontally and vertically, respectively, and the mainshell 32 regions horizontally due to its long length, 397.52cm. Such divisions in calandria shell are to obtain cell fluxes in each cell by using F4 tally, track length estimate tally.

In order to reduce the computer time required to obtain results with sufficient precision, several variance reduction techniques were used in this work: By using importance sampling, it is possible to spend more time for sampling in important regions such as the mainshell, annular plate, and the subshell and less time in unimportant regions. Energy cutoff technique was adopted to kill particles that have a energy out of the range of interest. The weight window technique, a space-energy-dependent splitting and Russian roulette technique, were also employed to keep the weight dispersion within reasonable bounds throughout the calcula-

Table 2. Material composition

Material	Element	Atomic Density [(atoms/barn-cm]
Core	H	1.097E-4
	D	5.638E-2
	O	2.825E-2
	Zr	1.443E-3
	U-235	8.605E-6
	U-238	1.187E-3
D_2O Reflector ($\rho=1.1/cm^3$)	H	1.839E-4
	d	6.599E-2
	O	3.309E-2
Vault Water(H_2O)	H	6.639E-2
	O	3.346E-2
Stainless Steel 304L ($\rho=7.9/cm^3$)	C	1.387E-4
	Si	1.271E-3
	Cr	1.734E-2
	Mn	1.732E-3
	Fe	5.812E-2
	Ni	8.107E-3
Stainless Steel 410 ($\rho=7.9/cm^3$)	Si	1.670E-3
	Cr	1.080E-2
	Mn	8.550E-4
	Fe	7.220E-4
Ordinary Concrete ($\rho=2.3/cm^3$)	H	9.583E-2
	C	1.143E-2
	O	4.531E-2
	Mg	6.018E-3
	Al	1.534E-4
	Si	1.783E-3
	Ca	7.498E-3
	Fe	1.112E-4
Ilmenite Concrete ($\rho=3.36/cm^3$)	H	4618E-3
	C	8.930E-4
	O	4.293E-2
	Mg	1.257E-3
	Al	2.598E-3
	Si	2.507E-3
	Ca	8.983E-3
	Fe	1.431E-4
Air[a]	O	4.536E-5

a. Treated as oxygen

tion.

The neutron cross-sections used in this MCNP runs were based on ENDL-85[5], ENDF/B-IV[6], and TMCCS files. The uranium cross-sections were extracted from ENDF/B-IV and other material cross-section data come form ENDL-85. The TMCCS files were used for thermal neutrons. The data in the TMCCS files represents thermal neutron scattering by molecules and crystalline solids. The upper energy bound used for thermal neutron tally was set to 0.414 eV for comparison of the results from DOT4.2.

CALCULATION OF PHOTON DOSE RATES AT ACCESSIBLE AREAS

The shield system of CANDU 6 reactor was modeled as shown in Figure 2 for MCNP runs to calculate the dose rates at various dose points outside the concrete vault walls during the reactor operation.

These points in details are shown in Figures 3 and 4 for the areas outside the primary side and the bottom shield, respectively. The dose points are located at the outer surface of the reactor wall concrete, the new fuel loading area, the stairway in the main lobby area, and main airlock area as shown in Figure 3. Figure 4 also shows eight specific dose points on contact with the bottom shield.

Gamma Dose rates are calculated as

$$D = \int_E DF_i(E)\phi(E)dE$$

where $DF_i(E)$ is the flux-to-dose-rate conversion factors from ANSI/ANS-6.1.1-1977(N-666)[7] and listed in Table 3 for photon. The conversion factors

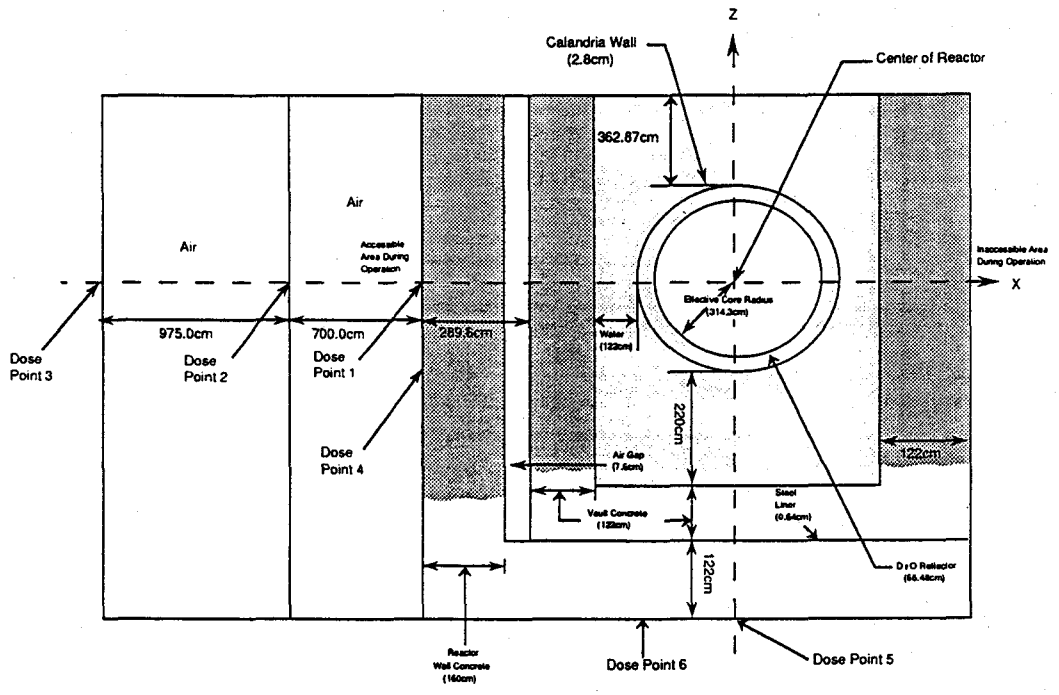

Figure 2. Calculation model for CANDU 6 shield system at Y=0.

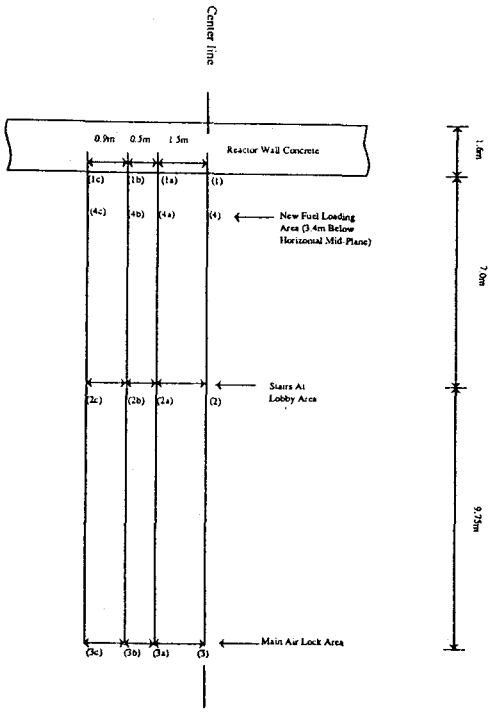

Figure 3. Detailed dose points outside reactor wall concrete.

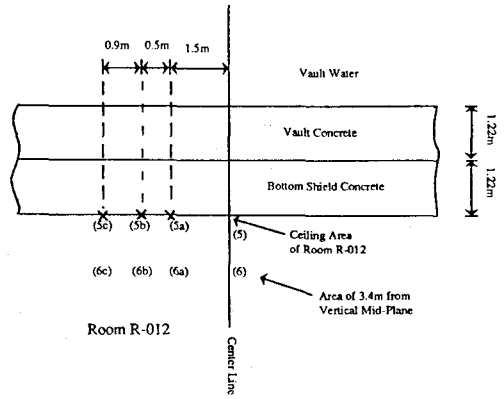

Figure 4. Detailed dose points outside bottom shield concrete.

Table 3. Gamma-ray flux-to-dose-rate conversion factors

Photon Energy E(MeV)	DF(E) (cSv/h)(photons/cm^2-sec)	Photon Energy E(MeV)	DF(E) (cSv/h)(photons/cm^2-sec)
0.01	3.96E-6	1.4	2.51E-6
0.03	5.82E-7	1.8	2.99E-6
0.05	2.90E-7	2.2	3.42E-6
0.07	2.58E-7	2.6	3.82E-6
0.1	2.83E-7	2.8	4.01E-6
0.15	3.79E-7	3.25	4.41E-6
0.2	5.01E-7	3.75	4.83E-6
0.25	6.31E-7	4.25	5.23E-6
0.3	7.59E-7	4.75	5.60E-6
0.35	7.87E-7	5.0	5.80E-6
0.4	9.85E-7	5.25	6.01E-6
0.45	1.08E-6	5.75	6.37E-6
0.5	1.17E-6	6.25	6.74E-6
0.55	1.27E-6	6.75	7.11E-6
0.6	1.36E-6	7.5	7.66E-6
0.65	1.44E-6	9.0	8.77E-6
0.7	1.52E-6	11.0	1.03E-5
0.8	1.68E-6	13.0	1.18E-5
1.0	1.98E-6	15.0	1.33E-5

are used with the DE(dose energy) and DF(dose function) cards to convert from a flux tally to a dose tally. The gamma flux can be obtained by using F5 tally, point detector tally, and then the dose rates are directly estimated from the formula. The log-log interpolation modes between energies and flux-to-dose conversion factors are used.

The photon weight card and detector contribution card were used together with the variance reduction technique in the calculation of thermal neutron flux distributions in calandria. The purpose of using the photon weight card is to control the number and weight of neutron-induced photons produced at neutron collisions. The detector contribution card reduces the number of contributions to point detector tallies from cells away many mean free paths from the detectors, thus can save computing time. The energy cut-off for lower energy photon is 0.01 MeV. The MCPLIB file based on the data of Storm and Israel[8] is used for photon cross-section table.

RESULTS AND DISCUSSION

The thermal neutron flux distributions for (n,

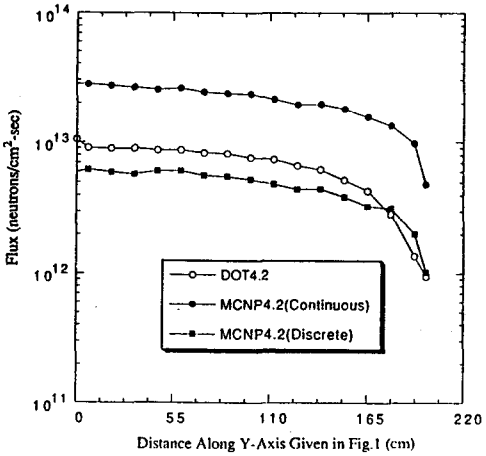

Figure 5. Thermal neutron flux distributions in the calandria mainshell.

Table 4. Thermal neutron flux distributions in calandria mainshell

Interval Along Y-Axis (cm)	Thermal Neutron Flux (neutrons/cm²-sec)	Interval Along Y-Axis (cm)	Thermal Neutron Flux (neutrons/cm²-sec)
−198.76～−186.33	4.90E+12	0～12.42	2.77E+13
−186.33～−173.92	1.01E+13	12.42～24.85	2.70E+13
−173.92～−161.49	1.45E+13	24.85～37.27	2.62E+13
−161.49～−149.07	1.65E+13	37.27～49.69	2.52E+13
−149.07～−136.65	1.87E+13	49.69～62.11	2.58E+13
−136.65～−124.22	2.05E+13	62.11～74.54	2.41E+13
−124.22～−111.80	2.29E+13	74.54～86.96	2.36E+13
−111.80～−99.38	2.33E+13	86.96～99.38	2.33E+13
−99.38～−86.96	2.42E+13	99.38～111.80	21.3E+13
−86.96～−74.54	2.45E+13	111.80～124.22	1.94E+13
−74.54～−62.11	2.82E+13	124.22～136.65	1.95E+13
−62.11～−49.69	2.60E+13	136.65～149.07	1.80E+13
−49.69～−37.27	2.63E+13	149.07～161.49	1.57E+13
−37.27～−24.85	2.72E+13	161.49～173.92	1.34E+13
−24.85～−12.42	2.62E+13	173.92～186.33	9.75E+12
−12.42～0	2.81E+13	186.33～198.76	4.81E+12

γ)reaction in calandria wall were calculated by using MCNP4.2 code. In this work, relative error, R, is less than 0.05 which is generally reliable for all tallies. The results at mainshell, annular plate, and subshell are given in Tables 4 through 6 and plotted in Figures 5 through 7, respectively. The results calculated by DOT4.2 code[2] with P_3 order of scattering and S_6 order of angular quadratures are plotted together with the MCNP4.2 results. From these results, it can be seen that the MCNP 4.2 results based on continuous cross sections give considerably higher values than that calculated by

Table 5. Thermal neutron flux distributions in calandria annular plate

Interval Along Z-Axis (cm)	Themal Neutron Flux (neutrons/cm²-sec)
340.68~343.42	7.79E+13
343.42~349.01	4.48E+13
349.01~354.61	3.05E+13
354.61~360.21	2.11E+13
360.21~365.80	1.47E+13
365.80~371.40	9.77E+12
371.40~377.00	5.91E+12
377.00~382.59	2.55E+12

Table 6. Thermal neutron flux distributions in calandria subshell

Interval Along Y-Axis (cm)	Themal Neutron Flux (neutrons/cm²-sec)
−297.18~−285.11	5.42E+12
−285.11~−273.04	9.99E+12
−273.04~−260.97	1.40E+13
−260.97~−248.90	1.78E+13
−248.90~−236.84	2.21E+13
−236.84~−224.78	2.75E+13
−224.78~−212.72	3.27E+13
−212.72~−198.76	4.92E+13
198.76~212.72	4.74E+13
212.72~224.78	3.30E+13
224.78~236.84	2.77E+13
236.84~248.90	2.28E+13
248.90~260.97	1.77E+13
260.97~273.04	1.32E+13
273.04~285.11	8.54E+12
285.11~297.18	4.61E+12

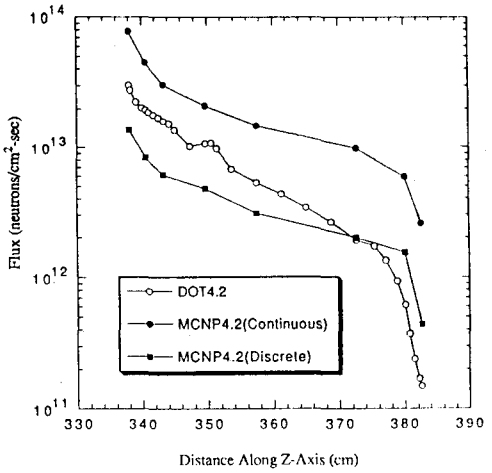

Figure 6. Thermal neutron flux distributions in the calandria annular plate.

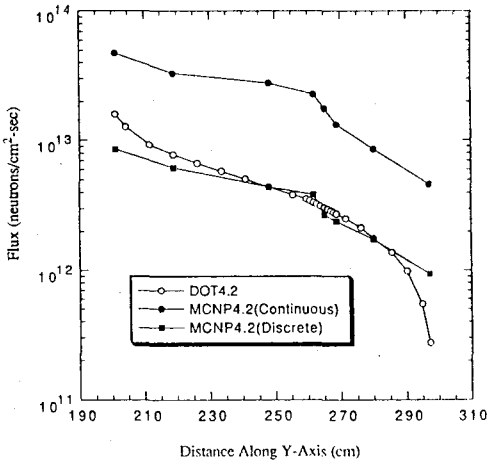

Figure 7. Thermal neutron flux distributions in the calandria subshell.

DOT4.2 with discrete cross sections. The differences between MCNP4.2 and DOT4.2 results may be caused by the different cross-section data set. For comparison, MCNP4.2 calculations using a discrete cross-section data, D9, were also carried out in the calandria shell, and the results are also plotted in Figures 5 through 7. Though D9 is different from the cross-section data used in DOT4.2 calculations, the results show a good agreement with that of DOT4.2.

As an application to the calculation of thermal neutron flux distributions in calandria shell, photon dose rates at the accessible areas in CANDU 6 were calculated by using MCNP4.2 code. Operating core gamma rays including fission product decay gamma rays do not contribute much to the dose rates at various dose points outside the concrete vault walls.

Table 7. Dose rates at accessible areas in CANDU 6 reactor

Dose Points	Dose Rates(μ Sv/h)
1	0.27
1a	0.15
1b	0.095
1c	0.042
2	0.10
2a	0.079
2b	0.069
2c	0.052
3	0.03
3a	0.028
3b	0.027
3c	0.024
4	0.015
4a	0.0011
4b	0.00042
4c	0.000047
5	0.71
5a	0.42
5b	0.25
5c	0.10
6	0.053
6a	0.0045
6b	0.0017
6c	0.0002

The calculated results at 24 dose points are given in Table 7. It can be seen that the dose rate at ceiling area of room R-012 is 0.71 μSv/h, the highest of all dose rates. The dose rates at the main airlock and new fuel loading areas as shown in Figure 3, which should be low considering frequent occupancy of these areas during reactor operation, are 0.03 μSv/h and 0.015 μSv/h, respectively. The calculated dose rates at all dose points of accessible areas meet a design target of CANDU 6 reactor, 6 μSv/h.

CONCLUSIONS

In CANDU reactor shielding analyses, it is very important to confirm the neutron fluxes in calandria and the photon dose rates at the accessible areas.

The new approach by MCNP 4.2 is able to carry out full scope calculation of CANDU 6 reactor system. It is worth to note that the thermal neutron fluxes obtained in this work showed higher values than that calculated by shielding analysis method curretly being used. In addition, as the photon dose rates calculated by MCNP 4.2 are much lower than the design target of CANDU 6 reactor, economic costs are to be diminished by reducing the concrete wall thickness.

The Monte Calro calculation used in this work can be applied to radiation shielding analysis of

other reactor types such as PWR as well as CANDU reactor.

REFERENCES

1. LASL Group X-6, "MCNP-A General Monte Carlo Code for Neutron and Photon Transport", Version 4, Los Alamos Scientific Laboratory, 1991.
2. K. Y. Kim and J. K. Kim, "Radiation Shielding Calculation on Sheild System of CANDU 6 Plant Using the Coupled DOT 4.2 and QAD-CG Codes" *J. of the Korean Nuclear Society,* Vol. 25, No. 4, December 1993.
3. A. L. Wight and R. Sibley, *Fuel Management Design Program-FMDP,* AECL Report TDAI-105, Atomic Energy of Canada Limited, Mississauga, Ontario, 1977.
4. G. D. Joanou and J. S. Dudek, *GAM-II, A B_3* Code for the Calculation of Fast-Neutron Spectra and Associated Multigroup Constants, GA-4265, General Atomics, 1963.
5. R. J. Howerton, *The LLL Evaluated Nuclear Data Library(ENDL): Evaluation Techniques, Reaction Index, and Descriptions of Individual Evaluations,* URCL-50400, Vol. 15, Part A, Lawrence Livermore National Laboratory, 1975.
6. R. Kinsey, *Data Formats and Procedures for the Evaluated Nuclear Data File, ENDF,* BNL-NCS-50496(ENDF-102), Brookhaven National Laboratory, 1979.
7. ANS Working Group 6.1.1, *Neutron and Gamma-Ray Flux-to-Dose Rate Factors,* ANSI/ANS-6.1.1-1977(N666), American Nuclear Society, 1977.
8. E. Storm and H. I. Israel, *Photon Cross Sections from 0.001 to 100 MeV for Elements 1 Through 100,* LA-3753, Los Alamos Scientific Laboratory, 1967.

몬테칼로 코드를 이용한 중수로 Calandria에서의 (n, γ) 반응유발 열중성자속분포 계산

김순영 · 김종경 · 김교윤*

한양대학교 원자력공학과
한국원자력연구소*

요 약

CANDU 6 중수형 원자로 운전중에 Calandria Shell 내에서 발생하는 (n, γ) 반응유발 열중성자속분포와 CANDU 6 발전소의 측면 및 하단 차폐구조에서의 방사선 선량률을 계산하기 위하여 몬테칼로 방법을 이용한 MCNP 4.2 코드를 사용하였다. 계산결과, Mainshell, Annular Plate와 Subshell내의 열중성자속분포는 10^{11}~10^{13} neutrons/cm^2-sec로 나타났고, 이는 DOT 4.2 코드의 계산결과와 비교해 볼 때 약간 큰 값들의 분포를 보여주고 있다. 이 계산결과의 응용으로서 작업자 접근가능지역(Worker Accessible Areas)에서의 감마 선량률을 계산해본 결과 설계목표치인 6μSv/h 보다 낮은 값을 주는 것으로 나타났다. (n, γ) 반응유발 열중성자속분포에 대한 MCNP 4.2 코드의 계산결과는 CANDU 6형 원자로의 방사선 차폐해석에 중요한 자료로 널리 이용될 수 있을 것이다.

중성자 : MCNP 4.2 코드, (n, γ)반응, 열중성자속분포, calandria, 감마 선량률, 작업자 접근가능지역